Journal of Himalayan Earth Sciences Volume 2026, No., 2026 pp. 01-14

Environmental Dynamics and Land Cover Change in Kotri, Pakistan: A 35-year NDVI Assessment

Muhammad Awais[1], Hadi Bux[1*], Arooba[1], Aasma[1], Ghulam Zehra[1] and Sonia Mumtaz[1]

[1] *Institute of Plant Sciences, Faculty of Natural Sciences, University of Sindh, Jamshoro 76080, Pakistan*

**Corresponding Email: hadiqau@gmail.com*

Submitted Date:22/05/2026 Acceptance Date: 24/06/2026 Publication Date:

Abstract

Land cover change is critical in semi-arid landscapes, and has significant implications for ecosystem services, agricultural management and water-resource planning. Local scale assessments are limited, but Kotri Taluka in the lower Indus Basin, Pakistan is ecologically and agriculturally important and has a long history of need for long term assessment at that scale. The land cover change was quantified in the Kotri Taluka from 1990 to 2025 using multi-date NDVI classification in Landsat. Five images were acquired during the monsoon season: one Landsat 4-5 TM in 1990, and four Landsat 8-9 OLI in 2013, 2020, 2022 and 2025, were classified as water, non-vegetated land, sparse vegetation, agriculture and dense vegetation. The area change of each class was computed and two-proportion z-tests were used to compare proportional changes between 1990 and 2025. Non-vegetated land decreased from 89,740 ha (61.12%) in 1990 to 65,002 ha (44.30%) in 2025, a 27.6% relative decrease ($p < 0.001$). Agriculture increased from 4,965 ha (3.38%) to 15,292 ha (10.40%), a 208% relative increase ($p < 0.001$). Total vegetation increased from 35.72% to 53.43%, a net gain of 25,960 ha ($p < 0.001$). Sparse vegetation increased by 13,587 ha (+30.4%, $p < 0.001$), while dense vegetation increased by 2,046 ha (+72.2%, $p < 0.01$). The analysis by period revealed non-linear dynamics: growth between 1990-2013, a decline between 2013-2020 and a rise again between 2020-2025. The results are baseline data for land use planning, agricultural sustainability and water resource management in Lower Indus Basin.

Keywords: NDVI time series; Environmental dynamics; Landsat; Indus Basin

1. Introduction

Land cover change is one of the most significant environmental changes that has occurred, or is occurring, on a global scale due to human activities and climatic variability. The transformation of natural landscapes into agricultural, urban and other uses has increased, and is having a significant impact on ecosystem services, biodiversity and regional climate (Almalki et al., 2022). Since the early 1970s, remote sensing has proven to be essential for land cover monitoring on spatial and temporal scales, allowing systematic observations. Low-frequency satellite observations are very useful for detecting changes in the environment which take place over a longer time period, and help to separate changes from inter-annual variations.

From remote sensing data, the Normalized Difference Vegetation Index (NDVI) is the common way to measure the greenness and photosynthetic activity of vegetation. NDVI is a good proxy for vegetation density, health and phenological state (Mancino et al., 2020). Landsat is optimal for long-term assessments due to its 30m resolution and 40-year archive. The cross-sensor comparison has been made possible by the inter-calibration functions of Landsat 4-5 Thematic Mapper, Landsat 7 Enhanced Thematic Mapper Plus and Landsat 8-9 Operational Land Imager. Water and non-vegetated land through agriculture and dense vegetation, particularly in semi-

arid areas, are classified using NDVI-based classification systems.

Land use and land cover (LULC) changes in South Asia have been very fast due to population increase, intensification of agriculture and urbanization. Sarmah et al. (2018) reported seasonal greenness indices and summer monsoons contributing to vegetation dynamics and significant greening in irrigated crop areas. The Indus Basin is home to about 300 million people and is highly modified by canals, dams, flood control and other features (Atif et al., 2021). Between 1948-1962 and 1990-2004, there was around 7% increase worldwide in semi-arid lands, especially in the Eastern Hemisphere (Huang et al., 2016).

In Pakistan, land use change analysis shows significant changes in land use. In the south Punjab, the forest area has reduced by 31.03% and settlements have increased by 14.52% from 2000 to 2021 (Hu et al., 2023). During the period from 2001 to 2016, the urban area grew by 24% in the urban area and 23% in agriculture in Faisalabad (Farah et al., 2021). The land surface temperature showed negative correlation with NDVI in built up areas of Thatta District, which experienced significant growth in urban areas between 1991 and 2021 (Khan et al., 2025). In the Upper Indus basin, there was a 11% growth in vegetation cover and 2.1% growth in built-up area in 30 years, whereas barren land decreased by 8.5% (Rehman et al., 2022). The detailed long term assessment at taluka level is limited for the Lower Indus Basin even in the face of these studies.

Kotri Taluka, in Jamshoro District, Sindh is ecologically as well as economically important in Lower Indus Basin. Irrigated agriculture, riparian vegetation and settlements develop along the Indus River in a semi-arid environment with an annual monsoon rainfall of 150-250 mm. The region has been faced with recurrent floods where the average of days spent with stagnant water in the lower basin is 425 days after major flood, reaching up to almost 800 days in certain areas (Atif et al., 2021). Agricultural intensification practices have been encouraged all over Pakistan (Jabbar et al., 2020). But systematic quantification of land cover change in Kotri Taluka for 30 years duration has not been done using remote sensing. All the previous studies carried out in Sindh were either done in coastal districts or basin scale flood dynamics, without any study on Kotri district.

Despite having a strategic location and being subjected to anthropogenic/climatic stress, there is no comprehensive assessment of land cover for Kotri Taluka that is based on NDVI data spanning 35 years. Previous research has focused on larger-scale or smaller-scale time spans. There is a lack of longitudinal information, which limits evidence-based planning. NDVI-based classification, however, is not able to identify non-vegetated land or built up areas because they have similar NDVI values. For this reason, these are grouped together as one non-vegetated class.

This study aimed to achieve three goals. First, to quantify land cover change in the Kotri Taluka area from 1990 to 2025 based on Landsat derived NDVI classification, areal estimates of five land cover classification were made: water, non-vegetated and built-up land (combined data), sparse vegetation, agriculture and dense vegetation. Second, to recognize the important transitions over the 35-year time span and test for statistical significance with two-proportion z-tests. Third, to explore changes over four sub-periods (1990-2013, 2013-2020, 2020-2022, and 2022-2025) to describe non-linear trends and switches in vegetation. This finding will be useful to understand the dynamics of land cover in the semi-arid Lower Indus Basin landscape in order to meet the objectives of the study, which will have implications for agriculture sustainability, water resource management, and adaptation to climate change in Pakistan.

The study was done in Kotri Taluka of Jamshoro District, Sindh Province of Pakistan (About 25.43°N, 68.28°E) (Fig. 1).

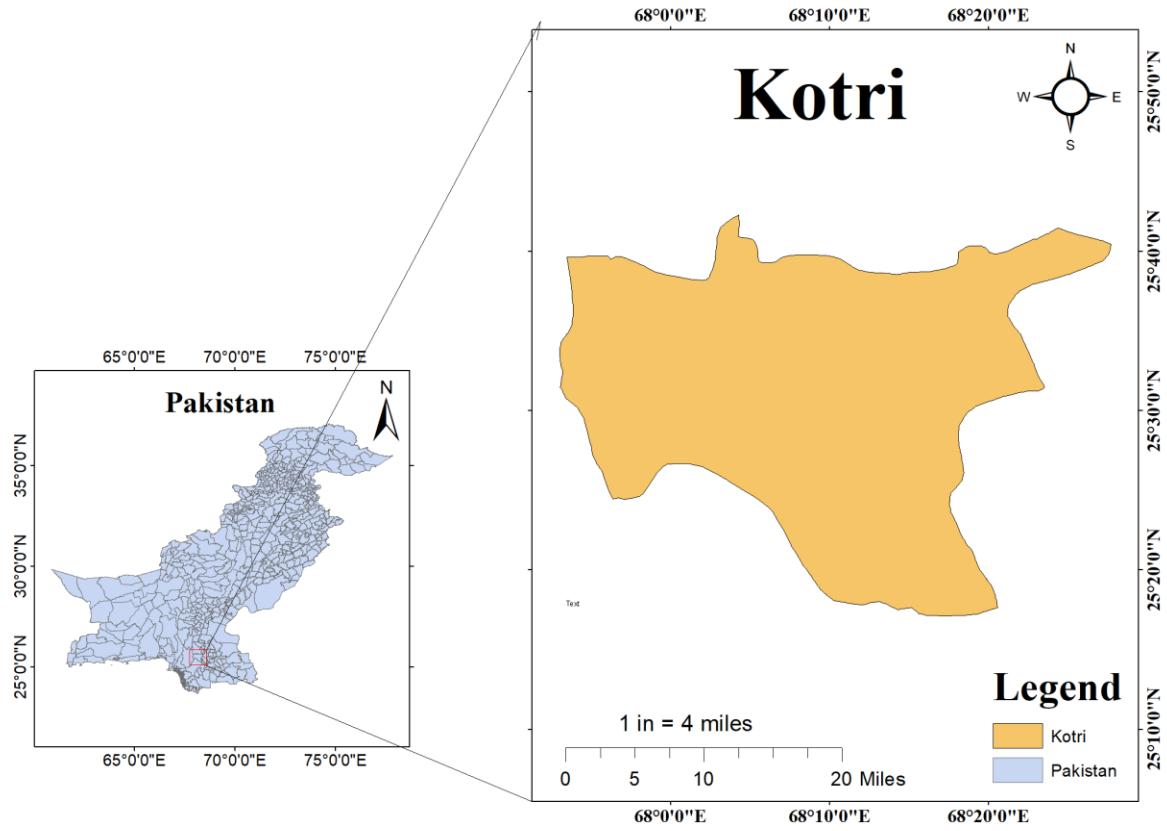

Fig. 1. Study area map showing Kotri Taluka in Jamshoro District, Sindh Province, Pakistan.

The overall study area is 146,834 ha. It has a semi-arid climate and an annual rainfall ranging between 150–250 mm, mainly occurring during the monsoon season (July–September). Its study area is traversed by the Indus River, upon which are located irrigated farms, riparian vegetation, and human settlements. Historically the natural land cover was comprised of non-vegetated land, and sparse xerophytic vegetation, with dense vegetation along the Indus River corridor. Regional land use is comprised of subsistence and commercial agricultural fields, rural settlements, and industrial land related to the city of Kotri. The boundary of the study area was defined by Sindh Province administrative boundaries from spatial database, and remained same throughout all analysis years for temporal consistency.

2. Methodology

2.1. Methodological Workflow

The overall methodology used in the present study is represented on a sequential flowchart from satellite data acquisition to the generation of the final output as shown in Figure 2. The workflow comprises of seven steps: (1) acquisition of Landsat data; (2) pre-processing: atmospheric correction, cloud masking, clipping to the boundary of the study area; (3) calculation of NDVI from the red and near-infrared bands; (4) classification of land cover based on the NDVI thresholds; (5) area calculation (hectares and percentages); (6) statistical analysis (two-proportion z-tests and period-wise relative change analysis); and (7) generation of final outputs (maps, tables, and summary statistics). These are explained in Figure 2.

2.2. Satellite Data Acquisition

Landsat satellite imagery was acquired for five time points: 1990, 2013, 2020, 2022, and 2025 (Table 1). Images were all chosen in the monsoon season (July-August) to maintain seasonality and to reduce phenological differences in the vegetation indices.

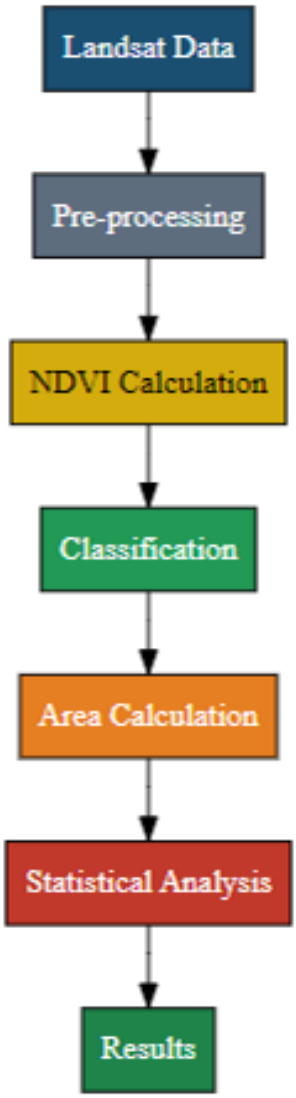

Fig. 2. Methodological flowchart of the NDVI-based land cover classification workflow for Kotri, Pakistan.

The United States Geological Survey (USGS) EarthExplorer portal (https://earthexplorer.usgs.gov) was the source for all images. Landsat 4-5 Thematic Mapper (TM) data were used for the 1990 image. Landsat 8 Operational Land Imager (OLI) data were used for the images of 2013 and 2020. The Landsat 8-9 OLI data were used for the 2022 and 2025 images. The spatial resolution of all images was 30 meters and was preserved across all sensors, to ensure comparability of pixel-based analyses. Subsequent vegetation index calculation used the red band and the near-infrared (NIR) band: with Landsat 4-5 TM, the red band (Band 3, 630–690 nm) and NIR band (Band 4, 760–900 nm); with Landsat 8-9 OLI, the red band (Band 4, 640–670 nm) and NIR band (Band 5, 850–880 nm).

To ensure cross-sensor comparability, all images were atmospherically corrected, and the same NDVI formula was applied. Strong cross-sensor agreement for NDVI between TM and OLI has been demonstrated (Wulder et al., 2022) though residual variation may contribute to uncertainty.

2.3. NDVI Calculation

Each image was also processed to calculate the Normalized Difference Vegetation Index (NDVI) as a numerical indicator of how green the vegetation and how much it is capable of photosynthesis. NDVI is a dimensionless index between −1 and +1 derived from reflectance bands in the red and near-infrared (NIR) spectra. The index takes advantage of the difference in the absorption of chlorophyll in the red band and of the leaf reflectance in the NIR band. The NDVI was computed for the Landsat-4/5 TM image from 1990 according to the following Equation (1):

$$\text{NDVI} = \frac{(\text{Band 4} - \text{Band 3})}{(\text{Band 4} + \text{Band 3})} \quad \text{……..(1)}$$

where Band 4 corresponds to the NIR band (760–900 nm) and Band 3 corresponds to the red band (630–690 nm).

For all Landsat 8 and Landsat 8-9 OLI images (2013, 2020, 2022, and 2025), NDVI was calculated using the following Equation (2):

$$\text{NDVI} = \frac{(\text{Band 5} - \text{Band 4})}{(\text{Band 5} + \text{Band 4})} \quad \text{……..(2)}$$

where Band 5 corresponds to the NIR band (850–880 nm) and Band 4 corresponds to the red band (640–670 nm).

NDVI computation was performed in ArcGIS using the Raster Calculator tool, which generated a continuous NDVI raster layer for each of the five time points. To avoid division-by-zero errors, a small constant (1×10^{-6}) was added to the denominator for all calculations.

Table 1: Satellite imagery used for land cover classification (Kotri Taluka, 1990–2025).

Year	Satellite	Sensor	Bands Used	Resolution	Source
1990	Landsat 4-5	TM	Band 3 (Red), Band 4 (NIR)	30 m	USGS
2013	Landsat 8	OLI	Band 4 (Red), Band 5 (NIR)	30 m	USGS
2020	Landsat 8	OLI	Band 4 (Red), Band 5 (NIR)	30 m	USGS
2022	Landsat 8-9	OLI	Band 4 (Red), Band 5 (NIR)	30 m	USGS
2025	Landsat 8-9	OLI	Band 4 (Red), Band 5 (NIR)	30 m	USGS

2.4. Overall Land Cover Changes

The continuous NDVI rasters were then categorised into five land cover classes based on NDVI threshold values obtained from spectral signature analysis and verified using high resolution Google Earth imagery at representative sample points. The classification system aimed to identify the predominant land cover types in the Kotri Taluka, which include: (1) water, (2) Non-vegetated land, (3) sparse vegetation, (4) agriculture, and (5) dense vegetation. The NDVI thresholds for each class are given in Table 2.

Table 2: NDVI thresholds used for land cover classification (Kotri Taluka, 1990–2025).

Class	Land Cover Type	NDVI Range
1	Water	< –0.11
2	Non-vegetated	–0.11 to –0.05
3	Sparse Vegetation	–0.05 to 0.01
4	Agriculture	0.01 to 0.12
5	Dense Vegetation	> 0.12

Water (Class 1) was identified by NDVI values less than –0.11, which reflect high reflectance in the red band and very low reflectance in the NIR band typical of clear or turbid water bodies. The NDVI values of both types of land cover in areas without vegetation are very similar, ranging between -0.11 and -0.05. Thus, all combined non-vegetated areas (Class 2) were grouped and separation of bare soil from built-up was not feasible by only relying on NDVI. It is recognized that this limitation exists and in this study the class is defined as non-vegetated land. Low NDVI values (Class 3) characterized sparse vegetation, which are indicative of little photosynthetic activity associated with overgrazed rangelands or early successional stages. Agriculture (Class 4) fell within a medium NDVI range (0.01 – 0.12), which corresponds to the growing season in the monsoon. NDVI values greater than 0.12 were classified as dense vegetation (Class 5) representing vigorous, healthy vegetation, such as mature riparian forests, well-established orchards or perennial vegetation along the Indus river corridor.

Reclassification was done in ArcGIS using the Reclassify tool. The results consisted of a categorical land cover image for each year (1990, 2013, 2020, 2022, 2025) with each 30 m x 30 m pixel classified to one of five land cover categories.

2.5. Area Calculation

The amount of area covered by each land cover class was determined for each time point. For a particular class, the area in hectares was calculated as shown in Equation (3), given that each pixel corresponded to an area on the ground of 30 m x 30 m = 900 m^2.

$$\text{Area (ha)} = N_{\text{pixels}} \times 0.09 \quad \text{.....(3)}$$

where N_{pixels} is the number of classified pixels belonging to that class and 0.09 is the conversion factor from 900 m^2 to hectares (1 ha = 10,000 m^2). The percentage of total area occupied by each class was calculated as follows: Equation (4):

$$\text{Percentage (\%)} = \left(\frac{\text{Class Area (ha)}}{\text{Total Area (ha)}}\right) \times 100 \quad \text{.....(4)}$$

The total study area was constant at 146,834 ha across all years, as the same boundary polygon was applied to all rasters. The area calculations were performed using the Zonal Histogram tool in ArcGIS, and the

results were exported to tabular format for subsequent statistical analysis.

2.6. Statistical Analysis

All the statistical analyses were carried out using R (version 4.3.2, The R Core Team, Vienna, Austria). A significance threshold of $\alpha = 0.05$ was adopted for all tests, with p-values reported as *p < 0.05, **p < 0.01, and ***p < 0.001.

2.6.1. Two-Proportion Z-Tests

Two-proportion z-tests were conducted to see if the changes in proportions of land cover classes from 1990 to 2025 were statistically significant. The relative size of land cover class (p_1990 vs. p_2025) were compared for each land cover class of interest. The null hypothesis was that the two proportions were equal (p_1990=p_2025). The test statistic was computed using Equation (5):

$$z = \frac{\hat{p}_{1990} - \hat{p}_{2025}}{\sqrt{\hat{p}(1-\hat{p})\left(\frac{1}{n_{1990}} + \frac{1}{n_{2025}}\right)}} \quad \text{.....(5)}$$

Where $\hat{p}_{1990}$ and $\hat{p}_{2025}$ are the sample proportions (class area divided by total area), $\hat{p}$ is the pooled proportion calculated as $(\text{area}_{1990} + \text{area}_{2025})/(\text{total area}_{1990} + \text{total area}_{2025})$, and n_{1990} and n_{2025} are the total number of pixels (which were equal across years). The resulting p-values were two-tailed. The comparisons included: Non-vegetated land (1990 vs. 2025), Agriculture (1990 vs. 2025), Total Vegetation (Sparse + Agriculture + Dense) (1990 vs. 2025), Sparse Vegetation (1990 vs. 2025), and Dense Vegetation (1990 vs. 2025). The p-values from two-proportion z-tests are not considered statistical inference statements because satellite pixels are not independent. In this study, the main evidence of change magnitude will be its effect sizes (percentage-point changes).

2.6.2. Period-Wise Relative Change Analysis

The relative changes for three aggregated classes (non-vegetated land, Agriculture, Total Vegetation (Sparse + Agriculture + Dense)) were calculated for each period, to characterize the temporal trajectory of land cover change with higher temporal resolution. For each consecutive period (1990–2013, 2013–2020, 2020–2022, and 2022–2025), the relative percentage change was calculated as Equation (6):

$$\text{Relative Change (\%)} = \left(\frac{A_{\text{end}} - A_{\text{start}}}{A_{\text{start}}}\right) \times 100 \quad \text{.....(6)}$$

Where A_{start} and A_{end} are the areal extents (ha) at the beginning and end of each period, respectively. Positive values indicate an increase, while negative values indicate a decrease.

2.7. Accuracy Assessment

The accuracy assessment was carried out to assess the reliability of the land cover classification of 2025 based on NDVI. The number of validation points were 50 with each of the five land cover classes (Water, Non-vegetated land, Sparse vegetation, Agriculture, Dense vegetation) having 10 validation points. A classified map class was compared with the actual land cover type interpreted from the high resolution Google Earth Pro imagery for each point. The accuracy attained by the users was determined for each class, and classification accuracy was determined as the percentage of points correctly classified from the total number of validation points.

2.8. Transition Matrix Analysis

A transition matrix was created to assess the level of change from one land cover to another at a pixel level between 1990 and 2025. The Tabulate Area tool in ArcGIS (Spatial Analyst Tools → Zonal → Tabulate Area) was used to compare the 1990 and 2025 classified rasters. This tool calculates the number of pixels that changed from each land cover class in 1990 to each class in 2025. The results were exported to MS-Excel where the number of pixels were converted to hectares by multiplying with 0.09 (as each pixel of 30m x 30m was equal to 0.09 ha). The consistency of the row and column totals was checked by comparing them to the class areas given in Table 3. The diagonal elements of the matrix are the areas that did not change

class, and the off-diagonal elements are the areas that changed class. Because NDVI does not adequately differentiate the type of bare soil from built-up surfaces, they were classified as one Non-vegetated land class. This limitation is applicable to all conversions between this class and other classes, and it should be treated as changes in low-vegetation surfaces, not specific conversions from bare soil to built-up land.

Table 3: Land cover change in Kotri, Pakistan between 1990 and 2025 showing areal extent (hectares), percentage of total area, and absolute and relative change for five land cover classes.

Land Cover Class	1990 (ha)	1990 (%)	2025 (ha)	2025 (%)	Change (ha)	Change (%)
Water	4,648	3.17	3,423	2.33	-1,225	-26.4
Non-vegetated	89,740	61.12	65,002	44.30	-24,738	-27.6
Sparse	44,646	30.41	58,233	39.70	+13,587	+30.4
Agriculture	4,965	3.38	15,292	10.40	+10,327	+208
Dense	2,835	1.93	4,881	3.33	+2,046	+72.2
Total	146,834	100	146,831	100	-	-

*Note: ha = hectares. Change (%) calculated relative to the 1990 extent. Total area remains stable at approximately 146,830–146,834 ha.**

2.9. Software

This used ArcGIS (version 10.8, Esri, Redlands, CA, USA), for all image pre-processing, NDVI calculation, classification and area calculation. Data were analyzed in R (version 4.3.2, R Core Team, Vienna, Austria) using statistical analyses such as two proportion z-tests and period-wise change calculations. Geographic information system and R (ggplot2 package) were used to create maps and figures.

3. Results

3.1. Spatial Overview

Classification maps derived from NDVI (Fig. 3) show the spatiotemporal change of land cover in the study area Kotri in the Lower Indus Basin for the time span of 1990-2025, which spans 35 years. The overall vegetation cover is highest in Figure 3a (2025), and is densest in the southernmost sections. After a decline, there has been renewed vegetation expansion in Figure 3b (2022). There is a partial reversal in 2020 compared to 2013 (Fig. 3c) as there are more areas of non-vegetated land exposed and less vegetation cover. Substantial greening is observed with the scattered of vegetation in central and southern parts and the expanded agriculture in Figure 3d (2013). Figure 3e (1990) depicts a landscape with little vegetative cover and few patches of vegetation, mostly occurring along riparian corridors. The areal composition of the five land cover classes is summarized and shown at each of the five time steps in the stacked bar chart (Fig. 4).

3.2. Overall Land Cover Changes (1990–2025)

Analysis of Landsat-derived NDVI classifications revealed substantial land cover change across the approximately 146,834 ha study area between 1990 and 2025 (Table 3).

In 1990, non-vegetated land dominated the landscape (89,740 ha, 61.12%), followed by sparse vegetation (44,646 ha, 30.41%), agriculture (4,965 ha, 3.38%), water (4,648 ha, 3.17%), and dense vegetation (2,835 ha, 1.93%). By 2025, non-vegetated land decreased to 65,002 ha (44.30%), a net loss of 24,738 ha (-27.6%). Total vegetation (sparse + agriculture + dense) increased from 35.72% to 53.43% of the study area, a net gain of approximately 25,960 ha. Agriculture showed the largest relative increase (+208%, from 4,965 ha to 15,292 ha), followed by dense vegetation (+72.2%) and sparse vegetation (+30.4%). Water decreased by 1,225 ha (-26.4%). Total area remained stable at approximately 146,831–146,834 ha.

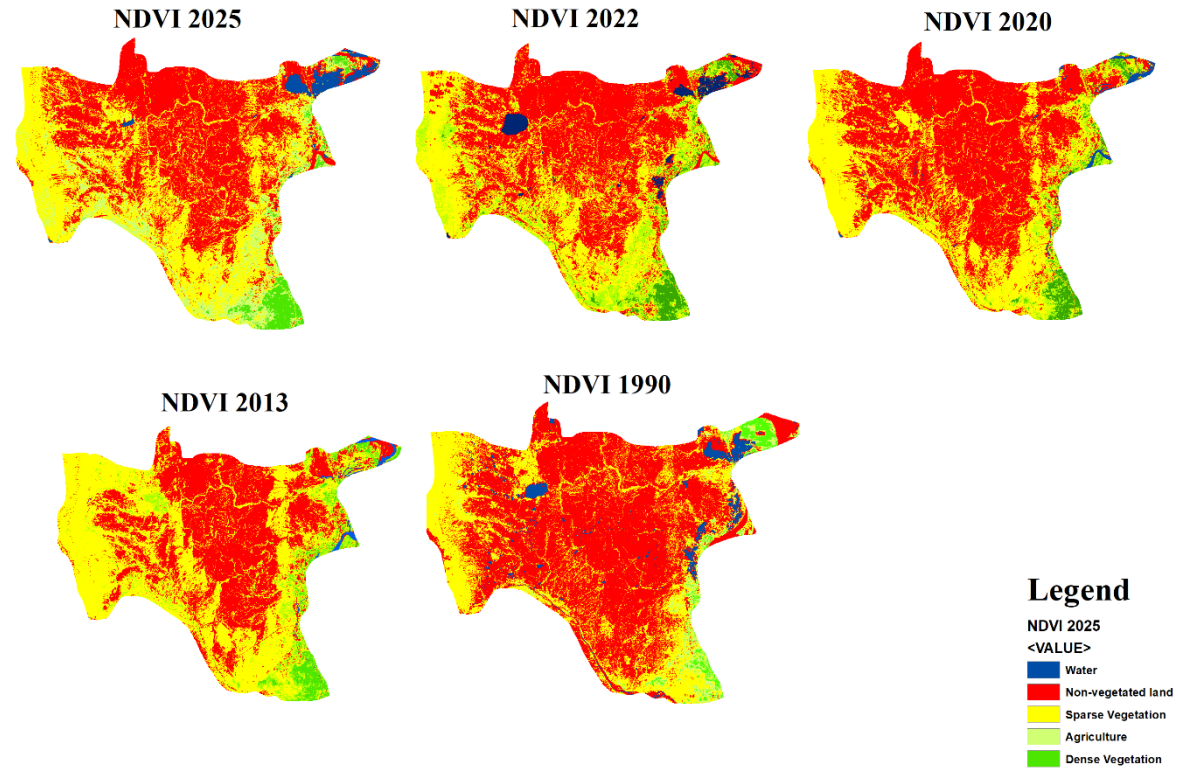

Fig. 3. NDVI-derived land cover maps of Kotri, Pakistan (1990–2025) showing (a) 2025, (b) 2022, (c) 2020, (d) 2013, and (e) 1990.

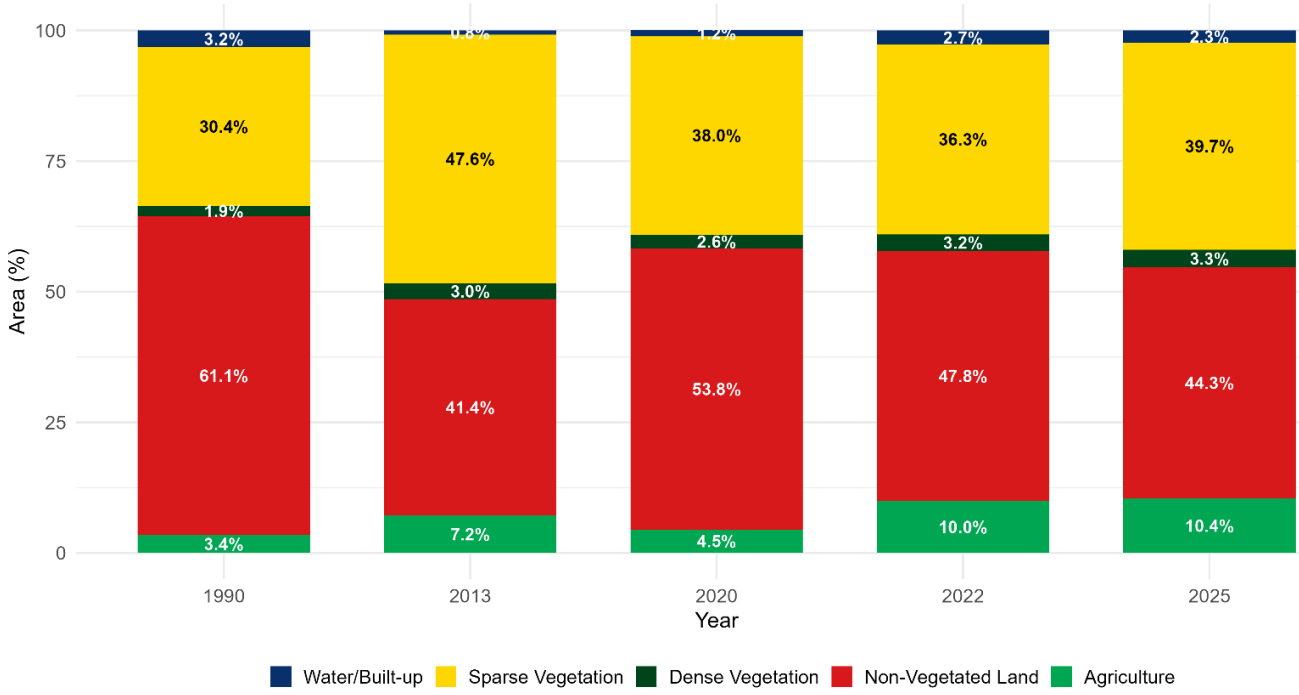

Fig. 4: Stacked bar chart showing land cover distribution in Kotri, Pakistan, from 1990 to 2025. Colors correspond to NDVI-derived classes as in Figure 3.

3.3. Statistical Significance of Changes

Two-proportion z-tests were performed to assess the robustness of the observed land cover transitions for proportions of land cover classes in 1990 and 2025 (Table 4). Overall, the decrease in the extent of land that was not vegetated was significant at the $p<0.001$ level. The expansion of Agriculture was also very important ($p < 0.001$). The total vegetation (Sparse+ Agriculture+ Dense) showed a very significant increase ($p<0.001$) when aggregated. Increase in Sparse Vegetation was also highly significant ($p < 0.001$) and Dense Vegetation increase was significant at $p < 0.01$. Two-tailed p-values are reported for all p-values.

3.4. Period-Wise Temporal Dynamics

Land cover change was not linear (Table 5), indicated by the changes over time. The largest changes between 1990 and 2013 were: A decrease in Non-vegetated land of 19.7% (based on the extent in 1990) and an increase in Total vegetation of 19.6%. During this early period agriculture grew slightly (+3.8% compared to 1990). There was a turnaround in 2013-2020. The total vegetated land decreased by 9.6%, and the non-vegetated land increased by 12.4% (relative to 2013). During this seven-year period, agriculture also experienced a decrease of 2.7%. The trend switched in 2020-2022, when non-vegetated land declined by 6.0%, and total vegetation grew slightly (+0.4%) and Agriculture grew by 5.5%. During the last period (2022-2025), Non-vegetated land further decreased (−3.5%), total vegetation grew (+3.1%) and Agriculture marginally grew (+0.4%).

3.5. Class-Specific Transition Patterns

The above net changes in land cover are a result of bi-directional changes, which are not captured in the net changes presented. The significant decrease in Non-vegetated land (−24,738 ha) and corresponding increase in Sparse Vegetation (+13,587 ha) and Agriculture (+10,327 ha) indicate a strong flow of land-use change from Non-vegetated land to the vegetated classes, especially in 2020-2025 and 1990-2013. A temporary rise in Non-vegetated land in 2013-2020 suggests that some of these changes are reversible. Despite being a smaller class in terms of absolute area, the Dense Vegetation class doubled in 35 years, reflecting the progressive greening in some areas, in keeping with the overall trend. The overall decrease in water/built-up was 1225 ha. The reduction could be due to reduction in open water, or because of a net loss of the pervious surface classes due to development of built-up areas.

3.6. Classification Accuracy Assessment

Accuracy assessment for the NDVI-based 2025 land cover classification was conducted using 50 validation points (10 per class) interpreted from high-resolution Google Earth Pro imagery. The user's accuracy for each class is presented in Table 6.

Table 4: Statistical significance of land cover changes in Kotri, Pakistan between 1990 and 2025 based on two-proportion z-tests.

Land Cover Class	Change (ha)	p-value	Significance
Non-vegetated land	-24,738	<0.001	***
Agriculture	+10,327	<0.001	***
Total Vegetation	+25,960	<0.001	***
Sparse Vegetation	+13,587	<0.001	***
Dense Vegetation	+2,046	<0.01	**

*Note: *** $p < 0.001$, ** $p < 0.01$. Two-proportion z-tests were applied to compare class proportions between 1990 and 2025. Total Vegetation includes Sparse Vegetation, Agriculture, and Dense Vegetation classes.*

Table 5: Period-wise relative changes in key land cover classes (Kotri, 1990–2025).

Period	Non-vegetated land Change (%)	Agriculture Change (%)	Total Vegetation Change (%)
1990–2013	–19.7	+3.8	+19.6
2013–2020	+12.4	–2.7	–9.6
2020–2022	–6.0	+5.5	+0.4
2022–2025	–3.5	+0.4	+3.1

Note: Percent changes are relative to the class extent at the beginning of each period.

Table 6: Accuracy assessment for the NDVI-based 2025 land cover classification.

Class	User's Accuracy (%)
Water	90
Non-vegetated land	90
Sparse vegetation	100
Agriculture	100
Dense vegetation	95
Overall Accuracy	95

The highest accuracies were observed for Sparse vegetation (100%) and Agriculture (100%), while the lowest was for Water and Non-vegetated land (90% each). The slightly lower accuracy for Non-vegetated land is attributed to the spectral similarity between bare soil and built-up surfaces, which NDVI alone cannot reliably separate. The overall classification accuracy of 95% indicates excellent performance for the NDVI-based approach.

3.7. Land Cover Transitions (1990–2025)

The transition matrix calculated from the NDVI data between 1990 and 2025 is shown in Figure 5. The diagonal cells show the areas of the same class and off diagonal cells show the areas converted.

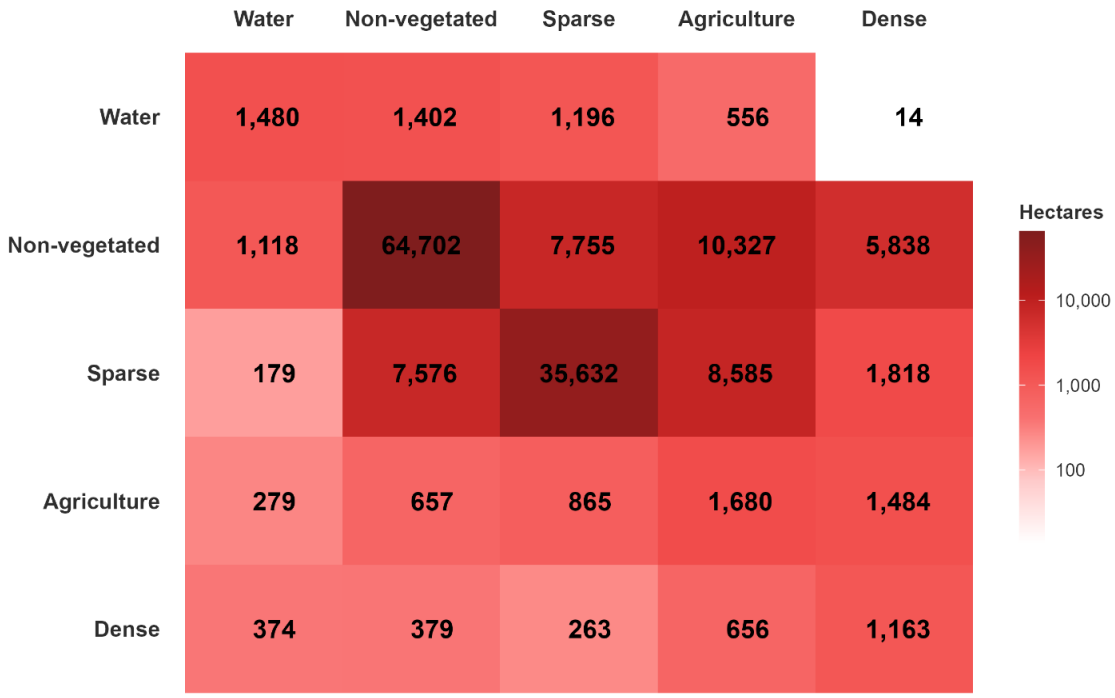

Fig. 5. NDVI-derived transition matrix heat map for Kotri Taluka (1990–2025). Rows represent 1990 classes; columns represent 2025 classes. Cell values = hectares converted. Darker red = larger area.

The most significant changes were between non-vegetated and agriculture (10,327 ha) and between non-vegetated and sparse vegetation (7,755 ha). The total area of non-vegetated classes decreased by 64,702 ha and the area of vegetated classes increased by 24,738 ha. Of particular note, there was some vegetation loss, with 7,576 ha of sparse vegetation becoming non-vegetated (browning). But 8585 ha of sparse vegetation were converted to agriculture and 1818 ha were converted to dense vegetation. These overall changes are corroborated by the matrix, which indicates that the net changes in Table 3, experienced by vegetation, were largely in the form of gains at the expense of non-vegetated surfaces. Built-up surfaces, and bare soil, are classified into the Non-vegetated land class, as it is not possible to discriminate between them from analysis of NDVI data alone.

4. Discussion

This study estimated the significant land cover changes for the Kotri Taluka during 35 years (from 1990 to 2025). Non-vegetated area decreased by 27.6% ($p < 0.001$), agriculture increased by 208% ($p < 0.001$), and total vegetation increased by 17.7% ($p < 0.001$). These net changes, however, masked a non-linear trajectory: greening (1990–2013), browning (2013–2020), and partial recovery (2020–2025). The overall accuracy of the classification based on the NDVI was 95% in the 2025 map, indicating the reliability of the data for change detection. The transition matrix showed that the agricultural expansion was mainly taking place at the expense of non-vegetated land (10,327 ha), with 7,755 ha being converted into sparse vegetation, which is in line with the observed greening shift. This agriculture growth of 208% is consistent with previous research findings of expanding cropland in the Indus Basin and Delta (Cheema et al., 2020; Masood et al., 2024). Such change has been seen in other areas of Pakistan, namely in Sindh and Bahawalpur, and is due to demographic pressure (Soomro et al., 2020; Arshad et al., 2022). But, agricultural expansion comes with sustainability concerns, as pointed by Kaur and Chauhan (2024) that monoculture cropping is a common feature of rapid agricultural expansion.

This net gain of vegetation cover (35.7% to 53.4%) is consistent with the findings of other continental scale studies (Mehmood et al., 2024; Rahman et al., 2025) which reported that NDVI increased considerably across Pakistan and South Asia due to variation in precipitation. The greening trend in Kotri is higher than the national average indicating that local factors have the ability to intensify the regional trend, which has been also observed in spate-irrigated regions of Sindh (Soomro et al., 2020). The browning reversal (2013-2020), however, shows vulnerability to climate variability. The decline in the amount of non-vegetated land (61.12% to 44.30%) shows a significant turnaround from the degradation pattern, which is in line with various studies conducted in different parts of Pakistan (Soomro et al., 2020; Arshad et al., 2022; Masood et al., 2024). A review on irrigation systems (Conrad et al., 2020) has been included to remind readers that in some cases, remote sensing can misrepresent complex patterns, and vegetation gains could be lost during 2013–2020 with the 12.4% increase in non-vegetated land.

For multi-decadal time series, there is the urgent need for the non-linear dynamics (1990-2013 greening; 2013-2020 browning; 2020-2025 recovery). However, similar non-linear dynamics have been reported in the Upper Indus Basin and in semi-arid China (Abbas et al., 2015; Liu et al., 2019), as well as agricultural land expansion and contraction due to environmental and economic factors (Hussain et al., 2022). Browning reversal can be due to commodity price changes, drought, or lesser availability of irrigation water. The high vegetation coverage rose from 1.93% to 3.33% (72.2% relative rise); this rise in plant cover is similar to that found in other reforestation impacts (Ali et al., 2024). The same vegetative multiplication and threats to the loss of crop diversity have been reported elsewhere (Masood et al., 2024; Kaur and Chauhan, 2024).

In the methodological aspects, the NDVI threshold method has been tested and proven in arid regions (Sun et al., 2018; Che et al., 2019; Islam et al., 2021). There was no formal accuracy assessment, however, because of the absence of ground truth data for early time points (1990 and 2013). Assessments are enhanced by field validation (Conrad et al., 2020). Limitations include: NDVI cannot distinguish between bare soil and built-up; no ground validation; mixed pixel misclassification; potential 2022 flood year spectral confusion; and no driver analysis. Future studies should include the collection of ground data, addition of NDBI, Sentinel-2 and integration of climate and socioeconomic data and modelling of future scenarios.

5. Conclusion

This study quantified the extent of land cover change in Lower Indus Basin, Kotri Taluka, having an area of about 1,468 km^2 from 1990 to 2025 by classifying the area into NDVI classes using Landsat data. Total vegetation increased from 35.7% of the study area in 1990 to 53.4% in 2025. The growth in agriculture was largest relative to the other categories (208%), and the reduction in non-vegetated land was the largest absolute relative to 2014 (27.6%). It was actually a non-linear trend, however, as it was a greening period from 1990 to 2013, followed by a browning period from 2013 to 2020 and partial recovery from 2020 to 2025. It demonstrates the need to monitor for long enough to differentiate between long-term trends and short-term fluctuations. The spatial trends seen are coherent with the agricultural expansion and greening of vegetation observed in the Indus Basin and South Asian region. But the non-linear dynamics also highlight the sensitivity of vegetation gains to inter-annual variation in climatic conditions and possible management disturbances. Bare soil was combined with built-up surfaces since these classes could not be separated with NDVI alone; this should be taken into account when interpreting transitions involving this class. The findings are part of the accumulating evidence on land cover change in Pakistan, and can serve as reference for future monitoring, land-use planning, agricultural sustainability and adaptation efforts for climate variability and change in the Lower Indus Basin. Further studies are needed to consider other spectral indices, higher resolution imagery, and environmental driver data to enhance classification accuracy and the interpretation of the driving mechanisms of observed changes.

Authors' Contribution

Muhammad Awais, proposed the main concept, designed the study methodology, performed all data processing and analysis including NDVI analysis, GIS-based analysis, satellite image processing, statistical analysis, preparation of figures, visualization of results, interpretation of findings, technical review, and manuscript preparation and final improvement before submission. Hadi Bux, supervised the research work, provided scientific guidance, contributed to manuscript review, and assisted in overall improvement of the manuscript. Arooba, Aasma, Ghulam Zehra, and Sonia Mumtaz contributed to data collection, literature review, identification of relevant references, manuscript writing, and revision of the manuscript.

Data Availability Statement

Datasets used in this study is available with the authors.

Conflicts of Interest

The authors declare no conflict of interest.

Declaration of Funding

This research received no specific funding from any public, commercial, or not-for-profit agencies.

References

Abbas, S., Qamer, F. M., Murthy, M. S., Tripathi, N. K., Ning, W., Sharma, E., & Ali, G. (2015). Grassland growth in response to climate variability in the Upper Indus Basin, Pakistan. *Climate*, *3*(3), 697-714.

Ali, M., Rahman, K. U., Ullah, H., Shang, S., Mao, D., & Han, M. (2024). Land reforestation and its impact on the environmental footprints across districts of Khyber Pakhtunkhwa in Pakistan. *Water*, *16*(20), 3009.

Almalki, R., Khaki, M., Saco, P. M., & Rodriguez, J. F. (2022). Monitoring and mapping vegetation cover changes in arid and semi-arid areas using remote sensing technology: A review. *Remote Sensing*, *14*(20), 5143.

Arshad, S., Hasan Kazmi, J., Fatima, M., & Khan, N. (2022). Change detection of land cover/land use dynamics in arid region of Bahawalpur District, Pakistan. *Applied Geomatics*, *14*(2), 387-403.

Atif, S., Umar, M., & Ullah, F. (2021). Investigating the flood damages in Lower Indus Basin since 2000: Spatiotemporal analyses of the major flood events. *Natural Hazards*, *108*(2), 2357-2383.

Che, X., Feng, M., Sexton, J., Channan, S., Sun, Q., Ying, Q., & Wang, Y. (2019). Landsat-based estimation of seasonal water cover and change in arid and semi-arid Central Asia (2000–2015). *Remote Sensing*, *11*(11), 1323.

Cheema, M. J. M., Khaliq, T., Liaqat, M. U., Khan, M. M., & Amin, H. (2020). Quantification of land use changes in complex cropping of irrigated Indus basin, Pakistan using MODIS vegetation time series data. *Pakistan Journal of Agricultural Sciences*, *57*(2).

Conrad, C., Usman, M., Morper-Busch, L., & Schönbrodt-Stitt, S. (2020). Remote sensing-based assessments of land use, soil and vegetation status, crop production and water use in irrigation systems of the Aral Sea Basin. A review. *Water Security*, *11*, 100078.

Farah, N., Khan, I. A., Abro, A. A., Cheema, J. M., & Luqman, M. (2021). The nexus of land use changes and livelihood transformation of farmers at rural-urban interface of Pakistan. *Journal of Rural Studies*, *87*, 216-228.

Hu, Y., Raza, A., Syed, N. R., Acharki, S., Ray, R. L., Hussain, S., & Elbeltagi, A. (2023). Land use/land cover change detection and NDVI estimation in Pakistan's Southern Punjab Province. *Sustainability*, *15*(4), 3572.

Huang, J., Ji, M., Xie, Y., Wang, S., He, Y., & Ran, J. (2016). Global semi-arid climate change over last 60 years. *Climate Dynamics*, *46*(3), 1131-1150.

Hussain, S., Qin, S., Nasim, W., Bukhari, M. A., Mubeen, M., Fahad, S., & Aslam, M. (2022). Monitoring the dynamic changes in vegetation cover using spatio-temporal remote sensing data from 1984 to 2020. *Atmosphere*, *13*(10), 1609.

Islam, H., Abbasi, H., Karam, A., Chughtai, A. H., & Ahmed Jiskani, M. (2021). Geospatial analysis of wetlands based on land use/land cover dynamics using remote sensing and GIS in Sindh, Pakistan. *Science Progress*, *104*(2), 00368504211026143.

Jabbar, A., Wu, Q., Peng, J., Zhang, J., Imran, A., & Yao, L. (2020). Synergies and determinants of sustainable intensification practices in Pakistani agriculture. *Land*, *9*(4), 110.

Kaur, S., & Chauhan, S. (2024). Dynamics of agricultural transformation in Punjab: Crop trends, instability and decomposition analysis. *Environmental Monitoring and Assessment*, *196*(9), 855.

Khan, A., Alamgir, A., & Fatima, N. (2025). Spatiotemporal analysis of land use and land cover changes, LST and NDVI in Thatta district, Sindh, Pakistan. *Kuwait Journal of Science*, *52*(1), 100326.

Liu, S., Huang, S., Xie, Y., Wang, H., Huang, Q., Leng, G., & Wang, L. (2019). Spatial-temporal changes in vegetation cover in a typical semi-humid and semi-arid region in China: Changing patterns, causes and implications. *Ecological Indicators*, *98*, 462-475.

Mancino, G., Ferrara, A., Padula, A., & Nolè, A. (2020). Cross-comparison between Landsat 8 (OLI) and Landsat 7 (ETM+) derived vegetation indices in a Mediterranean environment. *Remote Sensing*, *12*(2), 291.

Masood, M., He, C., Shah, S. A., & Rehman, S. A. U. (2024). Land use change impacts over the Indus Delta: A case study of Sindh Province, Pakistan. *Land*, *13*(7), 1080.

Mehmood, K., Anees, S. A., Muhammad, S., Hussain, K., Shahzad, F., Liu, Q., & Khan, W. R. (2024). Analyzing vegetation health dynamics across seasons and regions through NDVI and climatic variables. *Scientific Reports*, *14*(1), 11775.

Rahman, G., Farooq, U., Jung, M. K., & Kwon, H. H. (2025). Spatiotemporal vegetation dynamics in South Asia (2001-2023): Roles of climate and anthropogenic activities. *Geoscience Letters*, *12*(1), 31.

Rehman, A., Qin, J., Pervez, A., Khan, M. S., Ullah, S., Ahmad, K., & Rehman, N. U. (2022). Land-use/land cover changes contribute to land surface temperature: A case study of the Upper Indus Basin of Pakistan. *Sustainability*, *14*(2), 934.

Sarmah, S., Jia, G., & Zhang, A. (2018). Satellite view of seasonal greenness trends and controls in South Asia. *Environmental Research Letters*, *13*(3), 034026.

Soomro, A. G., Babar, M. M., Arshad, M., Memon, A., Naeem, B., & Ashraf, A. (2020). Spatiotemporal variability in spate irrigation systems in Khirthar National Range, Sindh, Pakistan. *Acta Geophysica*, *68*(1), 219-228.

Sun, H., Wang, Q., Wang, G., Lin, H., Luo, P., Li, J., & Ren, L. (2018). Optimizing kNN for mapping vegetation cover of arid and semi-arid areas using landsat images. *Remote Sensing*, *10*(8), 1248.

Wulder, M. A., Roy, D. P., Radeloff, V. C., Loveland, T. R., Anderson, M. C., Johnson, D. M., & Cook, B. D. (2022). Fifty years of Landsat science and impacts. *Remote Sensing of Environment*, *280*, 113195.